ATL-INDET-PUB-2008-010
01 July 2008

# A Study of TRT Noise in 2004 Test Beam Data

Thomas H. Kittelmann* and Esben B. Klinkby†

October 3, 2006

**Abstract**

In this note noise in the ATLAS Transition Radiation Tracker is analysed using data from selected runs from the June 2004 TRT standalone test beam. A procedure which reliably extracts noise hits is presented and the main features of those are examined. Finally, channel-to-channel correlations in noise levels are examined and the distribution of dead channels is compared to earlier module test bench results.

## 1 Introduction

Even though the noise level in the ATLAS Transition Radiation Tracker[1] (TRT) is known to be quite low, $\mathcal{O}(1\%)$, noise is still a relevant effect and as such ought to be both simulated along with the rest of the electronics response in the digitisation phase as well as accounted for in reconstruction algorithms.

The purpose of the present note is to provide a basis for such an inclusion in the simulation algorithms by analysing data from the 2004 TRT standalone test beam [LR04]. After a brief overview of the TRT read out digitisation scheme in section 1.1, its is demonstrated in section 2 how genuine noise hits are reliably extracted from the test beam data and the general characteristics of those are shown. Finally, in section 3 correlations between noise levels in different channels are investigated.

### 1.1 TRT Thresholds and Digitisation Scheme

The amount and time-structure of the energy deposited in a TRT straw when crossed by a particle, in principle holds a great deal of information regarding both the track and identity of the particle. For practical reasons the analog signal in the wire is digitised in the front-end electronics before it, given a level 1 trigger, is read out by the higher level triggers and possibly stored offline. More specifically, the analog signal treatment (amplification and shaping) as well as the analog to digital digitisation step is performed in the ASDBLR chips[2] while the links to the timing, trigger and read out systems are handled by DTMROC's.[3]

The analog to digital conversion is handled through implementation of two thresholds, a low threshold (LT) for tracking – approximately corresponding to the signal height produced

*The Niels Bohr Institute, University of Copenhagen. Email kittel@nbi.dk.
†The Niels Bohr Institute, University of Copenhagen. Email klinkby@nbi.dk.

[1] See e.g. [ATL97a] and [ATL97b].
[2] Short for Amplifier/Shaper/Discriminator with Baseline Restoration, cf. [B+96].
[3] Short for Drift Time Measuring Read Out Chip, cf. [A+01].

| Bit Pattern | HT | LT Bit Pattern | Typical cause |
|---|---|---|---|
| 0 00000000 0 00001111 0 11111000 | off | 000000000000111111111000 | Passing $\pi$ |
| 0 00000000 1 11111110 0 00000000 | on | 000000001111111000000000 | Passing $e$ |
| 0 00111110 1 00000011 1 11111110 | on | 001111100000001111111110 | $\pi$ followed by $e$ |

Table 1.1: Three examples of TRT digits and their typical physics causes.

by a single primary cluster with a minimum deposit of 300 eV – and a high threshold (HT) used for detecting the absorption of energetic photons emitted by electrons through transition radiation. The high threshold is usually set to about 5-7 keV.

For the LT every 25 ns time period, corresponding to one bunch crossing, is divided into eigth bins of approximately 3.125 ns (giving a resolution of $3.125 \text{ ns}/\sqrt{12} \approx 0.9$ ns), and for each bin a single bit is stored indicating whether the LT was exceeded (1) or not (0). Regarding the HT only one single bit is set for the whole period. Data is then read out in 75 ns segments, requiring a total of 27 bits per read out straw.

In this note the terminology will be that a digit has a HT if at least one of the three HT bits is set, and "bit pattern" will usually refer to the pattern of the 24 LT bits. A few examples of bit patterns are shown in table 1.1.

# 2 2004 Test Beam Data

In July 2004, 6 functional and tested TRT barrel modules, corresponding to 2 out of 32 phi sectors, were placed in the H8 test beam in the SPS North Area at CERN Prévessin. Using various targets and magnet field selectors, beams of either pions, electrons or muons were delivered. This was the first test beam with the front-end electronics (including the ASDBLR chips) essentially of the final design, while the readout chain and data acquisition system were final prototypes, very similar to the ones that will be used in ATLAS.

In figure 2.1.a the test beam setup is shown, with the beam entering from the left. The beam passed through various detectors in addition to the barrel modules. These additional detectors possessed abilities to do high quality particle identification, tracking and shower vetoing. Figure 2.1.b shows an example of a recorded pion event. The details of the setup and its performance are described in in e.g. [Tik04]. The setup thus provides events, where the identity of the passing particle is well known and with good external knowledge of the parameters of the passing track, thus making them suitable for detailed studies of detector performance.

For the present noise studies the type of beam should in principle not matter, but for cross-checking purposes three runs with different beam compositions and energies are selected as summarised in table 2.1 and figure 2.2.

## 2.1 Initial Selection of Noise Hits

The goal of the present study is to understand the rate and composition of the noise digits, i.e. the digits associated with the hits in figure 2.1.b, whose appearance are clearly not due to the passing track. Since the number of such noise digits over an entire run is rather high, quite safe cuts can be afforded, while keeping the statistics at a sufficient level.

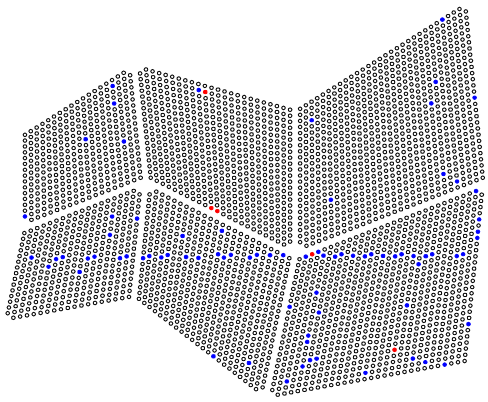

(a) (b)

Figure 2.1: Basic setup of the 2004 TRT standalone test beam (a), with indicated distances in mm, and an example pion event from run 3183 (b). Straws with HT passed are shown in red, while those with only a passed LT are shown in blue.

| Run number | Beam Energy | Electrons | Number of events |
|---|---|---|---|
| 3183 | 80 GeV | no | 90K |
| 3240 | 20 GeV | yes | 60K |
| 3241 | 20 GeV | yes | 80K |

Table 2.1: Beam types and number of events for the three runs of data taking used in this section. All of the runs were taken using low threshold values of approximately 300 eV, high threshold values around 7 keV and with the beam passing the modules roughly in the position shown by the track in figure 2.1.b. Note that the beams were not pure electron or pion beams in the strict sense, but contaminated to some extent – see figure 2.2.

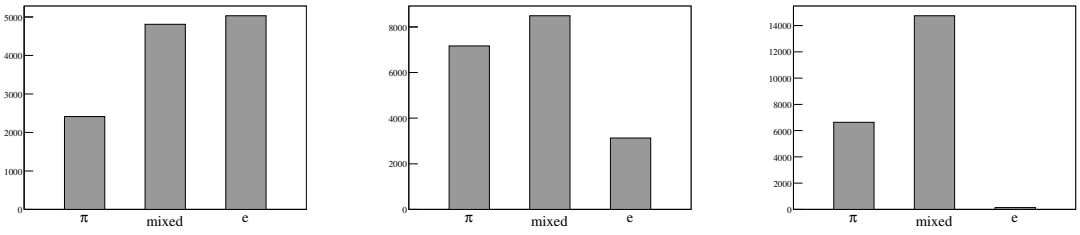


20 GeV $e$ (run 3240) | 20 GeV $\pi$ (run 3241) | 80 GeV $\pi$ (run 3183)

Figure 2.2: Beam compositions for the three investigated runs. The electron and pion identification was performed using external detectors and the remaining impurities are thought to be at a negligible level (although this is not essential for the present study). The central column denoted *mixed* simply refers to the events that were not identified as either electrons or pions under the given cuts.

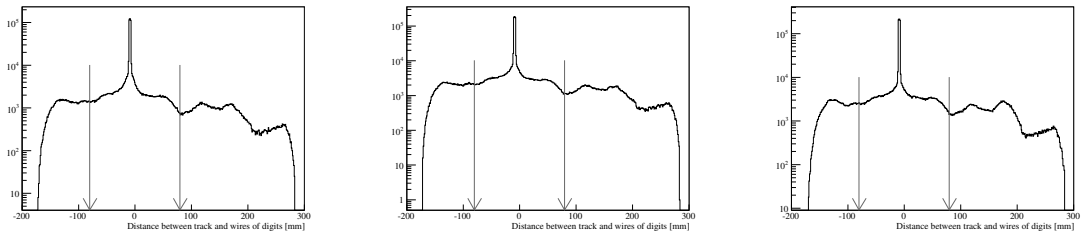


20 GeV $e$ (run 3240) | 20 GeV $\pi$ (run 3241) | 80 GeV $\pi$ (run 3183)

Figure 2.3: Illustration of the cut used to eliminate digits from straws too close to the track.

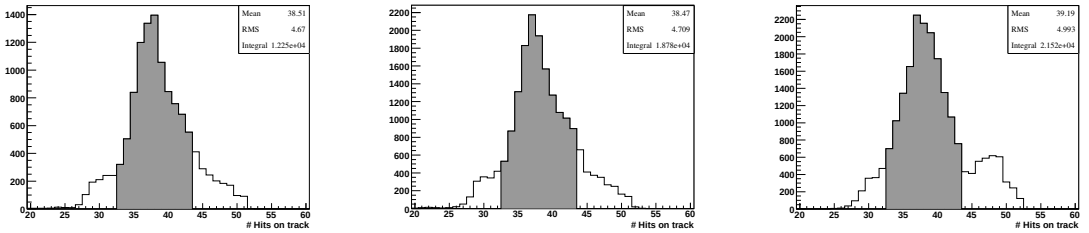


20 GeV $e$ (run 3240) | 20 GeV $\pi$ (run 3241) | 80 GeV $\pi$ (run 3183)

Figure 2.4: Distribution of number of hits that are classified as being "on track". The accepted ranges are indicated in grey.

The first and primary selection cut is to only consider digits originating from straws with wires located at a certain minimum distance away from the passing track. In addition to removing hits on the reconstructed track this cut must also ensure a high rejection of digits caused by secondary particles and "cross-talk" – i.e. wire currents induced through capacitive couplings to a genuine large current in a neighbouring wire. Finally, some events will have more than one beam particle, and since the typical vertical spread of the beam was around 3 cm, the cut must be much larger than this. The final value of the cut is determined by looking at the actual distribution of the distance between the wires of the digits and the reconstructed track as shown in figure 2.3. A cut of 8 cm is chosen as the tails from the track peak at zero seems to be negligible after this distance.

An additional way to ensure that the single track in the event is indeed single and well reconstructed, is to require the number of hits on the track not to deviate too much from the average number for a single track. As indicated by the greyed out regions in figure 2.4, the reconstructed track is required to have at least 33 and a maximum of 43 hits on track. In particular, the distribution in the 80 GeV pion run exhibits a small secondary peak around 48, which is probably due to multiple beam particles, and something the chosen cut avoids.

In addition, one should note that some digits have initially been disregarded by the requirement that it should be possible to identify at least one leading edge in the LT bit pattern. This simply means that bit patterns where the first LT bit is already on, e.g. `11111100000000000000000000` are discarded as they do not allow one to identify the time of the leading edge for tracking, since it could have occurred before the considered 75 ns interval. The exception to the rule is where a second leading edge is present as in e.g. `11110000000111111110000000`.

Finally, straws with a noise level higher than 15% (corresponding to a noise frequency of $0.15/75$ ns $= 2$ MHz) have been masked out. This is reasonable since such noisy channels will certainly be masked out in the final setup of the detector in ATLAS.

## 2.2 Removal of Hits in Abnormal Straws

The vast majority of noise digits are thought to originate from Gaussian fluctuations in thresholds and potentials in the various channels occasionally exceeding the low threshold and producing said noise. However, looking at the data one notices a few noise digits that clearly have another origin. This is for instance digits such as,

```
0 01111111 0 11111111 0 11111111 [a]
1 00000000 1 00000000 1 00000000 [b]
0 00000001 1 00000000 0 00000000 [c]
```

Here digit [a] is from a straw where the LT is almost always exceeded, indicating a major problem in that particular straw or front-end electronics. Such a straw will probably be masked in any case in the long run. Digit [b] shows a similar structure, but here the problem is in the high threshold. Finally, digit [c] shows an otherwise innocent noise digit with a high threshold in the second 25 ns time-slice, where somewhat mysteriously the low threshold was never exceeded. A possible explanation is that the noise digit was in reality `0 00000011 0 00000000 0 00000000`, but that the readout driver (ROD) was somehow off by one bit – a problem known to have occurred occasionally.

While these problems are real and present in the test beam data, there is no reason to believe that they will be sufficiently similar to the ones encountered in the full ATLAS running to make a detailed study sensible. Furthermore, they represent a relatively small fraction of the total number of noise hits. For these reasons the present studies will only try to understand and model the intrinsic noise of the apparatus and will not deal with these kinds of errors. In the following it will therefore be described how straws producing such "abnormal" digits can be identified and removed based on a statistical analysis of the digits they produce. To be meaningful this of course requires a minimum number of digits from each straw, and noise hits originating from straws, from which there are accumulated less than a total of 20 hits are therefore a priori ignored. This systematically throws away noise hits from the least noisy straws, but the alternative is to keep a few straws around with e.g. quite abnormal electronics. Given the low number of hits from these straws, neither choice is likely to affect the conclusions, as long as the overall noise level is not taken too literally. For simplicity the plots shown in this section will all be based on run 3240, although all runs have of course been examined.

The first quantity to consider, on a straw-to-straw basis, is the fraction of noise hits having at least one high threshold bit turned on. The high threshold is typically much higher than the low threshold (e.g. 7 keV versus 0.3 keV) and the frequency with which the low threshold is being exceeded by noise is low ($\mathcal{O}(1\%)$). This implies, given the naïve expectation of noise being generated by Gaussian fluctuations in electronics voltages and thresholds, that it is very unlikely that high thresholds will appear in noise hits, apart from those really caused by abnormal electronics and possibly stray tracks.

In figure 2.5.a the average high threshold fraction is shown for each of the remaining relevant straws. It is clear that not all straws give noise hits with negligible HT fractions, and that there is some structure caused by systematic differences between the channels (although

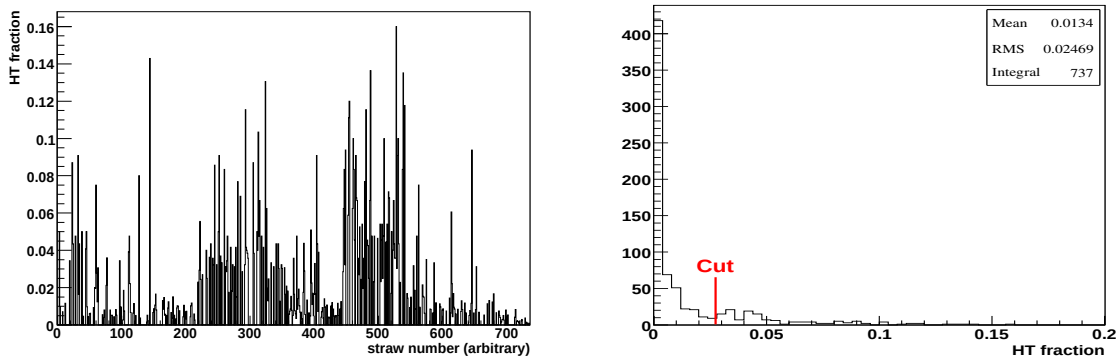


(a) (b)

Figure 2.5: Average high threshold fractions straw by straw (a), and their distribution (b). Around 10 straws had an observed HT fraction of exactly 1.0 and are not shown in either figure.

the straw numbering is somewhat arbitrary, it is still such that straws with numbers close to each other are usually placed close to each other in the detector). In figure 2.5.b the distribution of those same fractions is shown. As expected there is a huge peak around zero with a tail towards higher values, which is likely due to secondaries (the results in the next section seems to be in agreement with such an interpretation). However, at values around 0.04 there is again a peak, which is hard to interpret as anything else than straws with some sort of abnormal behaviour. One might be tempted to put in an aggressive cut just around the peak at zero, but could fear that such a cut would simply remove a genuine "non-abnormal" effect. Consequently, it is chosen to place the cut just before the peak, eliminating any straw with an average HT fraction above 0.028. Not surprisingly this gets rid of almost all of straws producing digits consisting almost entirely of 1's (which really is a sign of seriously flawed electronics).

Another indication that a straw is "abnormal" is if it often produces noise digits with a relatively large number of LT bits set. In figure 2.6.a is shown the distribution of the average number of set LT bits in the selected noise digits for each straw. The grey regions show how the straws with a HT fraction higher than respectively 6% and 2.8% are distributed. It shows that there is clear correlation between straws with a relatively large number of LT bits set and straws with a large HT fraction. This supports the claim that the source of noise in these straws is somehow "abnormal", if not simply contamination due to remaining real passing particles. Based on this knowledge, straws with an average of more than 3.0 set LT bits are discarded.

Finally, the distribution of noise levels of the individual remaining straws is shown in figure 2.7. Note that the removal of straws with less than 20 hits earlier has removed entries at the lowest values.

## 2.3 Noise Digit Features

Using the selected sample of noise digits, with the exclusion of contributions from "abnormal" sources, the features of the noise can be extracted. Regardless of the considered feature, its distribution ought to be essentially independent of beam type and run.

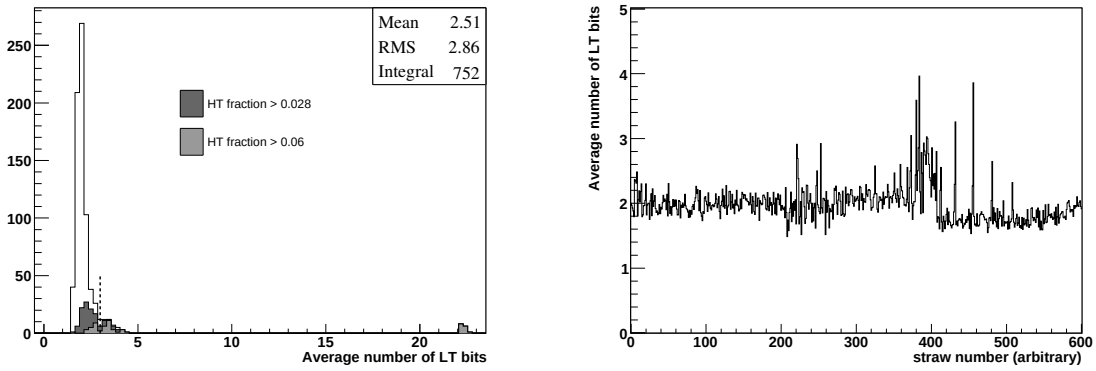


(a) (b)

Figure 2.6: Average number of low threshold bits that are set for each straw. Note that 24 set LT bits are an impossibility due to the requirement of a leading edge as discussed in the text, but some abnormal channels with 22-23 set bits appear. In (a), the distributions of straws with a high HT content are also indicated. In (b), only the straws with HT fraction $< 0.028$ are shown.

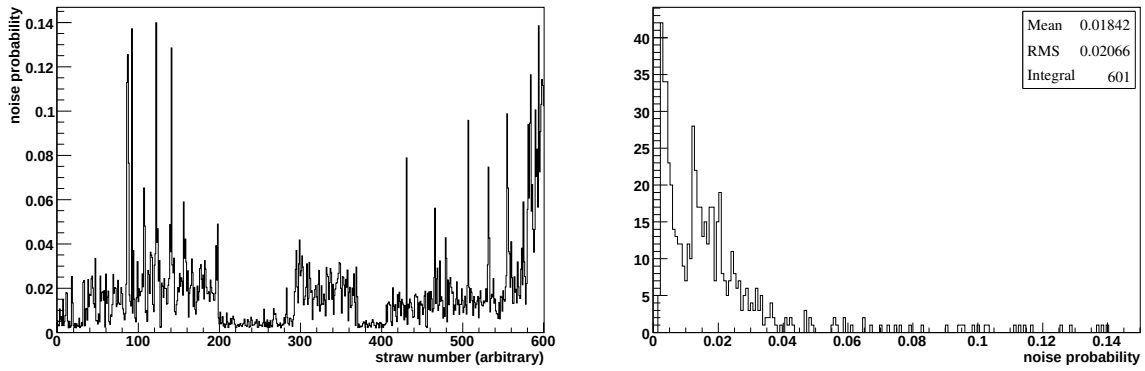


(a) (b)

Figure 2.7: Observed noise levels versus straw number (a) and the distribution of those numbers (b).

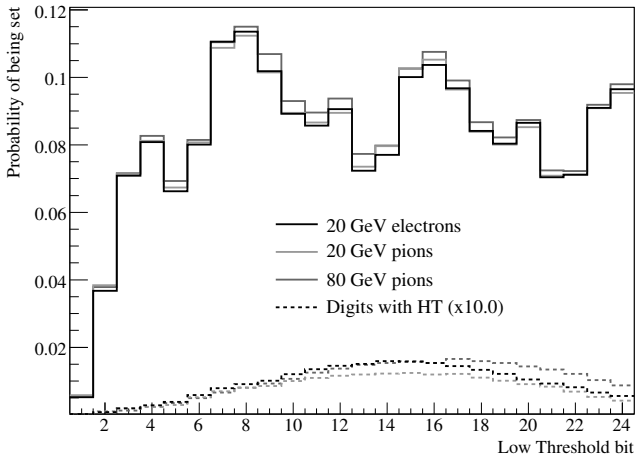


Figure 2.8: Solid histograms show the observed mean low threshold bit occupancy in selected noise digits for the three different runs. The dashed histograms show the contribution from digits with a high threshold – scaled up by a factor of 10 for better visibility.

The time structure of the noise can be investigated by plotting the mean occupancy of the 24 LT bits in noise digits as is done in figure 2.8. If, on average, the noise had no time structure, one would expect a flat distribution, but this is obviously not what is seen. First of all, there is a large dip in the early bins, which is easily understood as an artificial effect caused by the requirement of a leading-edge as discussed in section 2.1.

Apart from the dip there does seem to be some sort of plateau around 8-10% with a 8 bit (25 ns) periodic structure on top of it. This is not surprising since the front-end electronics is influenced by an externally driven 25 ns clock cycle. Also shown in the figure is the contribution which is due to digits with a HT. The very low number of these means that their contribution is too small to be of significance. Secondly, they have a different and in-time shape, not too different (if a little broader) from that of beam particles. This supports the hypothesis that the noise digits with HT content are likely due to stray beam particles or secondaries.

Perhaps the most striking feature of figure 2.8 is how robust the distributions seem to be across the three runs, which underlines the consistency of the entire procedure. Furthermore, it shows the stability of the detector conditions, which means that e.g. reconstruction and digitisation can improve performance by using appropriate calibration data updated at moderate intervals.

Figure 2.9 shows another extracted quantity, namely the distribution of the number of set low threshold bits, and it is seen that, in the selected noise digits, about 99% of the entries have 4 bits or less set, and the three runs agree completely regarding the distribution in those bins. Looking at the distribution for digits with a HT bit set, it again agrees with the hypothesis that there is a small and negligible contamination of stray particles and secondaries, thus explaining the present tail. If instead, for instance, the presence of set HT bits were caused by ROD off-by-one problems, one would expect the distribution of digits with HT to follow the overall distribution, apart from being shifted left by one.

The mean of the distribution corresponds to an average time above threshold around $1.96 \cdot 3.125$ ns $\approx 6$ ns, which is quite low compared to the time over threshold due to pulses from traversing particles that are usually around 15-35 ns, as shown in figure 2.9.b. This is

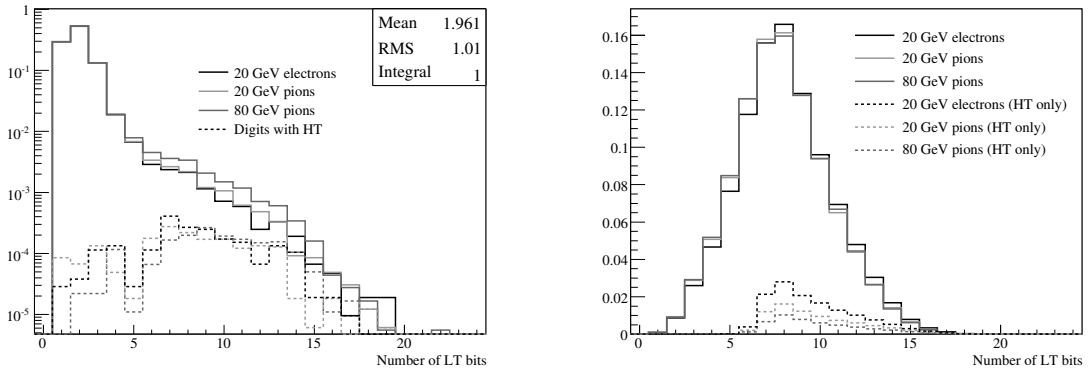


(a) (b)

Figure 2.9: The solid histograms in (a) show the distribution of the number of low threshold bits set in the selected noise digits, with the hashed histograms showing the small contribution of digits with a HT. In (b) the same distribution is shown for on-track digits.

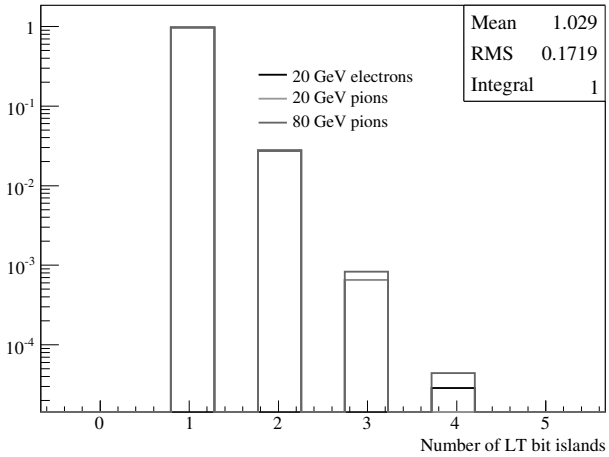


Figure 2.10: Distributions of the number of LT bit "islands" (or "trains") in the selected noise digits.

certainly a feature that could be used for reducing the impact of noise at just a small cost in tracking efficiency.

Finally, figure 2.10.b shows the distribution of the relative fractions of number of LT bit "islands" (also known as "trains"). An island is simply a group of set LT bits surrounded by unset bits (00000001100010000000000 thus contains two islands while 00111000000000000000000 contains only one). One notices that the relative suppression of the fraction of 2-island digits compared to 1-island digits is roughly equal to the one between 3 vs. 2 islands and 4 vs. 3 islands respectively, and that the suppression is comparable to the overall noise level of around 2%. This implies that the creation of noise fluctuations at separate times is uncorrelated to a good approximation.

# 3 Channel-to-Channel Correlations in Noise Levels

The distributions studied in the previous sections have all been based on the entire pool of (usable) channels. For a more complete understanding it is also necessary to study the channel-to-channel correlations caused by their various mechanical and electrical groupings. Channels are connected to different high voltage supplies, belong to different chips and are connected to wires in different barrel modules. More detailed, the obvious relevant groupings are:

- Groups of eight neighbouring wires are connected to the same ASDBLR chip, responsible for the analog treatment and digitisation of the potential fluctuations in the wires. The threshold values can not be tuned independently for each channel, but only overall for each ASDBLR chip.
- Two ASDBLR chips are connected to a DTMROC, responsible for collecting and, given a level 1 trigger, reading out the digitised results from the ASDBLR chips to the ROD's as well as keeping the clock synchronised with the overall ATLAS clock through interaction with the TTC (Trigger Timing Control) boards. Because it is merely an overhead to the ASDBLR pad groupings, correlations between the noise levels and the groupings of 16 channels connected to each DTMROC are not investigated.
- Groups of eight wires share a single high voltage connection and are denoted as "HV pad's".
- Several hundreds of straws and corresponding electronics are mechanically assembled into three types of barrel modules. Such barrel modules contain either 329, 520 or 793 straws and are accordingly denoted as type I, II or III (with type I modules closest to the beam axis).[4]

In the next sections, correlations and non-uniformities in the straw noise levels will be investigated at several levels. First, the module to module differences will be discussed in section 3.1. Next, in section 3.2, it is investigated how the individual straw noise levels are correlated with their groupings into sets of eight wires connected to the same HV pad. Finally, the relative distribution of straw noise levels within each HV pad is examined in section 3.3,

[4]While end cap elements were not present in the test beam it should be noted that the situation for those is not entirely the same, as each mechanical grouping of straws (into "wheels") contains a much larger number of straws and many more electronics boards.

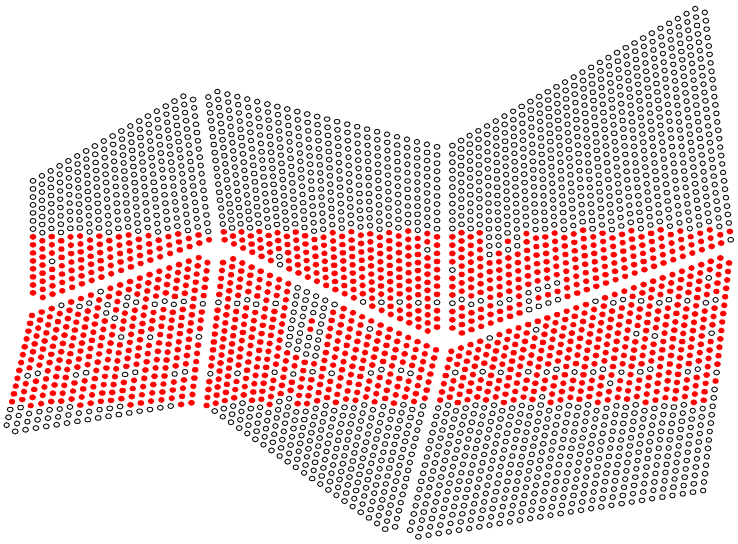

Figure 3.1: Straws illuminated by the beam (e.g. containing on-track hits) in any of the runs considered for the channel-to-channel noise level variation studies.

and in section 3.4 it is checked whether noise in one channel could give rise to noise in neighbouring channels.

For this analysis, several runs of test beam data were used in addition to the three considered in section 2. This was done because the beam position (cf. figure 2.1.b) was the same in all of the three runs considered so far, meaning that a large group of straws was excluded in every event solely by the distance to track cut. The inclusion of other runs with different beam positions alleviates this problem and allows for a more detailed picture of the noise, but of course care should be taken not to add samples which differ significantly in some way or another. A number of cross-checks showed no major deviations between the runs and the addition of different runs is considered safe. The difference in beam positions for all of the considered runs is illustrated by the beam illumination map shown in figure 3.1. Finally, the studies are complicated by the fact that some channels are excluded by the quality cuts discussed in section 2.2. This means in particular that not all HV pads will contain data from all eight channels, but rather some subset instead. Care is therefore taken to ensure that artifacts from this varying number of channels in each grouping are not mistaken from genuine statistical effects.

## 3.1 Module to Module Variations

In the full ATLAS setup there will be installed 96 barrel modules, whereas only 6 modules were present in the 2004 test beam setup.

In table 3.1 is shown the mean of the individual channel noise levels in each of the six modules. It is clear that there are significant module to module differences which is perhaps not very surprising considering that the six modules for various reasons are classified as "abnormal" based on the results from pre-installation high voltage and radiation tests [Gag05]. Also,

| | Module Type | | |
|---|---|---|---|
| | I | II | III |
| Upper Sector | 1.6% | 0.5% | 1.9% |
| Lower Sector | 0.3% | 0.3% | 0.3% |

Table 3.1: Mean of the noise levels of the individual channels within each of the six modules.

one should note that the low thresholds in the test beam setup were set similarly across all ASDBLR chips, whereas the plan for the configuration in the final ATLAS setup is to adjust the threshold for each chip such that the noise level averaged over its eight channels will be fixed at e.g. 2.25% (corresponding to a noise frequency of 300 kHz). This future configuration scheme will obviously limit the module to module variations in noise levels considerably but the variation will then instead occur in the variations of effective channel-to-channel low thresholds. Despite the module to module variations, the data from all of the six test beam modules are still equally useful for studying other relative channel-to-channel variations in the following sections.

## 3.2 The HV Pad Level

In order to investigate how individual channel noise levels are correlated with their groupings into pads, the distribution of the normalised mean noise levels of the pads, i.e. the mean of the noise levels of the (usable) straws within each pad normalised to the mean straw noise level of the containing module, is shown in figure 3.2.a. As one of the straw quality cuts explained in section 2 is a minimal number of noise hits, one might worry that errors are introduced when perfectly fine straws with extremely low noise levels are thrown away. As a cross-check two different distributions are shown in figure 3.2.a: One where only the straws considered for the noise studies within a pad is used to calculate the mean and one where in addition all the remaining straws are used with an assumed noise level of 0% (which will thus be different for pads with less than eight usable channels). Apart from a naturally enhanced first bin, the two methods seems to give compatible results. One should also note that the means of the distributions in figure 3.2.a are not equal to one as one might expect since the straw noise levels have been normalised to the average straw noise levels of the containing modules – the different pads does not contain the same number of (usable) straws, so the individual straws will contribute to the mean with a different weight depending on which pad they belong to. Hypothesising that straws with a high noise level will more often belong to pads where all straws are used than those with low noise level, one would indeed expect a mean lower than one.

It is difficult, however, to tell directly from the distributions in figure 3.2.a whether they indicate a significant correlation between straw noise level and pad groupings. In order to test this further a similar distribution was made in figure 3.2.b, but this time using randomised straw to pad groupings instead of the actual ones. It is indeed seen that the mean of the distribution approaches one, while the root-mean-square of the distribution decreases, which is also exactly what one would expect to happen when the pad groupings are randomised, effectively making the pads more similar on average. To test the significance of the results, the mean and root-mean-square the distributions for a hundred different randomised pad groupings are shown in figure 3.3. They show with high significance that a random pad

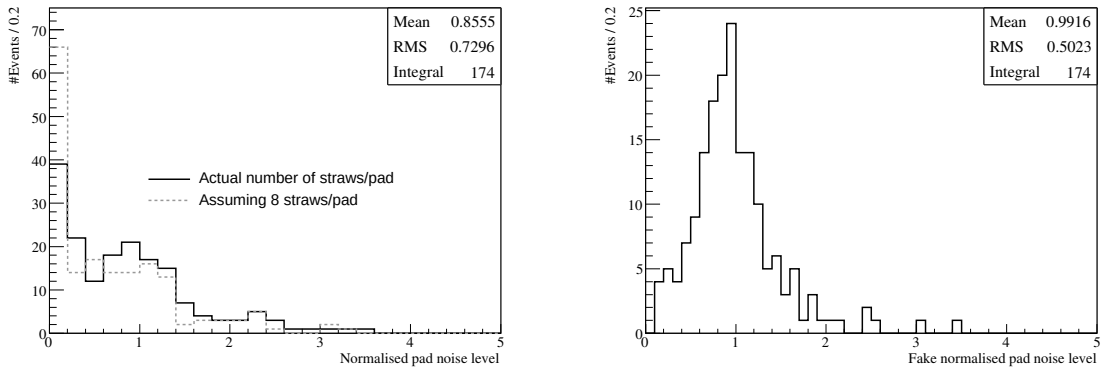


(a) (b)

Figure 3.2: In (a) is shown the distribution of the mean straw noise level within each pad, normalised to the average noise level of the containing module. Both the actual average of the used straws within each pad as well as the average after assuming all unused straws to be straws with a noise level of 0% are plotted. Figure (b) shows the same distribution, but the straw to pad assignment has been randomised.

grouping could never reproduce the distributions in figure 3.2.a.

## 3.3 The Straw Level

In figure 3.4 is shown the distribution of noise in straws normalised to the average noise in the pad to which the straw belongs. The distribution is peaked around unity with most entries within $[0.4, 1.5]$, which shows that the noise level of most straws is approximately the noise level of their corresponding pad, although of course the mean is guaranteed to be one by construction and the tail towards high values is not negligible. For potential use in the simulation it is noted that the distribution is well described when fitted by a Gaussian plus an exponential. To check that there is no significant biased introduced due to the fact that the number of considered straws within a given pad is not always eight (since some straws are disregarded by cuts) the same distribution is also plotted solely for pads with eight surviving straws. The distribution seems to be relatively unaffected by this requirement, with the most striking difference being the disappearance of the artificial peak at exactly 1.0 caused by pads for which only one channel were considered usable.

## 3.4 Noise Induced Channel-to-Channel Cross-Talk

A potentially important effect of is the possibility of cross-talk between straws, i.e. when a signal in one straw induces a signal in another straw through a capacitive coupling. This is potentially dangerous for track reconstruction as a signal due to a passing particle could give rise to a fake signal in a nearby straw. These issues are investigated in [TRT04]. Here it will instead be investigated whether a *noise* hit in one straw is likely to induce noise hits in nearby straws. A priori one would not expect this as the level of tracking induced cross-talk is known to be rather low and the energy deposited in a straw by a passing particle will usually be much higher than the one associated with a noise hit.

To estimate the magnitude of this effect from noise one can look at the number of noise

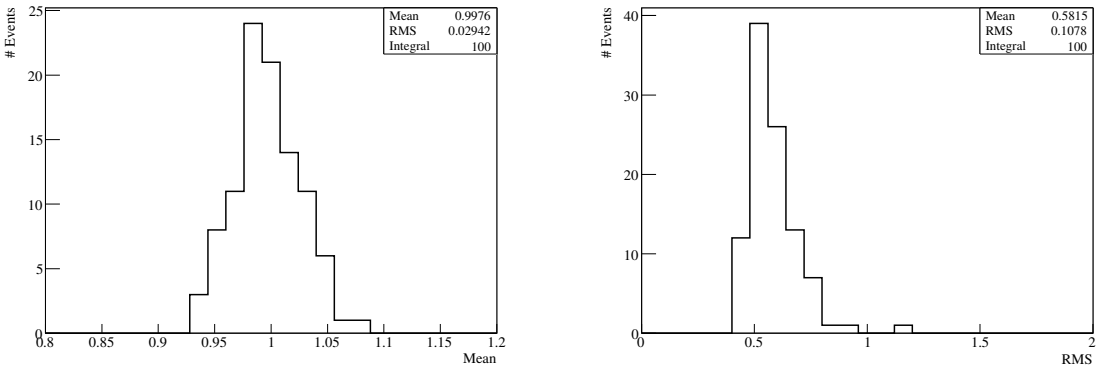


(a) (b)

Figure 3.3: In (a) and (b) respectively are shown the distribution of the means and root-mean-squares of 100 randomised straw to pad mappings such as the example shown in figure 3.2.b.

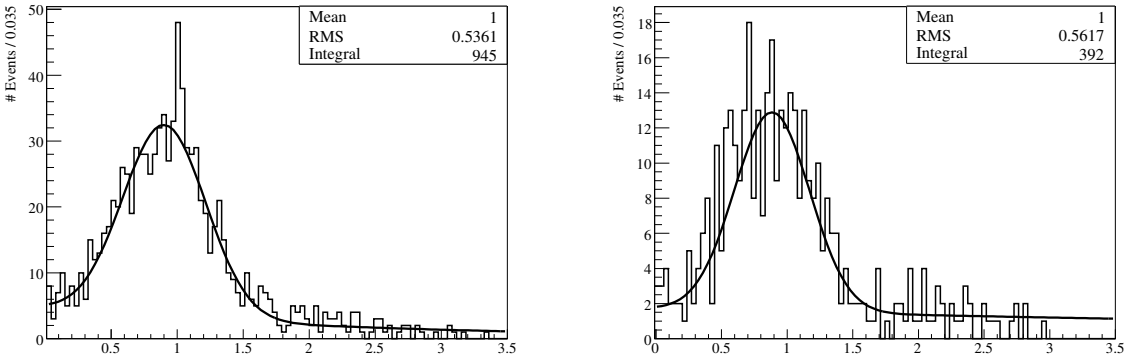


(a) (b)

Figure 3.4: Distribution of noise level in straws normalised to the average level in the pad to which the straw belongs for all pads (left) and for pads where all eight straws contribute (right).

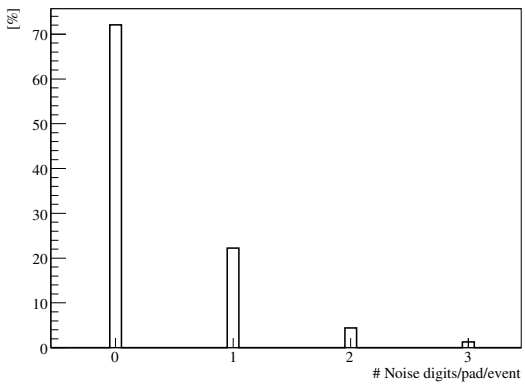


Figure 3.5: Number of noise hits in a given pad in a given event.

hits within a given pad in a given event, of course using the fact that straws connected to a given pad are located next to each other. The distribution is shown in figure 3.5, but only for pads where all eight straws are deemed usable. Assuming no cross-talk and similar noise levels in all straws, the ratio between the content of the $'1'$ and $'0'$ bins, $r_{10}$, should follow from binomial distributions:

$$r_{10} = \frac{N_{\text{ch}} p_{\text{nl}} \left(1 - p_{\text{nl}}\right)^{N_{\text{ch}}-1}}{\left(1 - p_{\text{nl}}\right)^{N_{\text{ch}}}} = \frac{N_{\text{ch}} p_{\text{nl}}}{1 - p_{\text{nl}}} \quad \Rightarrow \quad p_{\text{nl}} = \frac{r_{10}}{r_{10} + N_{\text{ch}}} \tag{3.1}$$

Where $p_{\text{nl}}$ is the probability for a noise hit in a given straw and $N_{\text{ch}} = 8$ the number of channels per pad. Likewise the expected ratio of the $'2'$ and $'0'$ bins is found to be:

$$r_{20} = \binom{N_{\text{ch}}}{2} \frac{p_{\text{nl}}^2 \left(1 - p_{\text{nl}}\right)^{N_{\text{ch}}-2}}{\left(1 - p_{\text{nl}}\right)^{N_{\text{ch}}}} = \binom{N_{\text{ch}}}{2} \frac{p_{\text{nl}}^2}{\left(1 - p_{\text{nl}}\right)^2} \tag{3.2}$$

If the assumption of truly independent channel noise is valid, a direct calculation of $r_{20}$ from the bin content in figure 3.5 should give the same result as first calculating $p_{\text{nl}}$ via equation 3.1 and inserting the result in equation 3.2. Inserting numbers the two methods turns out to result in $r_{20}^{\text{obs}} = 6.1\%$ and $r_{20}^{\text{indep}} = 4.2\%$ respectively. This thus reveals a slightly enhanced tendency to get two noise hits in the same pad, which could to some extent be explained by noise induced channel-to-channel cross-talk. However, it is still true that $r_{20}^{\text{obs}} \ll r_{10}^{\text{obs}}$, meaning both that the effect is relatively rare and it is difficult to conclude with any certainty that it is not simply caused by e.g. a small contamination of the noise hit samples from real particle induced hits.

## 3.5 Dead Channels

Another method of studying detector inhomogeneities is examination of the distribution of non-sensitive, or "dead", channels in the test beam setup. One would expect two major sources of such channels: The first being problems with individual channels and the second being possible problems in a chip connecting eight channels.

Already at the barrel test facility $\mathcal{O}\left(1\%\right)$ of all assembled straws were found to have serious and unrepairable problems. The causes were numerous: gas leaks, bend straws or abnormal wire tension, gain or high voltage behaviour. Consequently their anode wires were removed

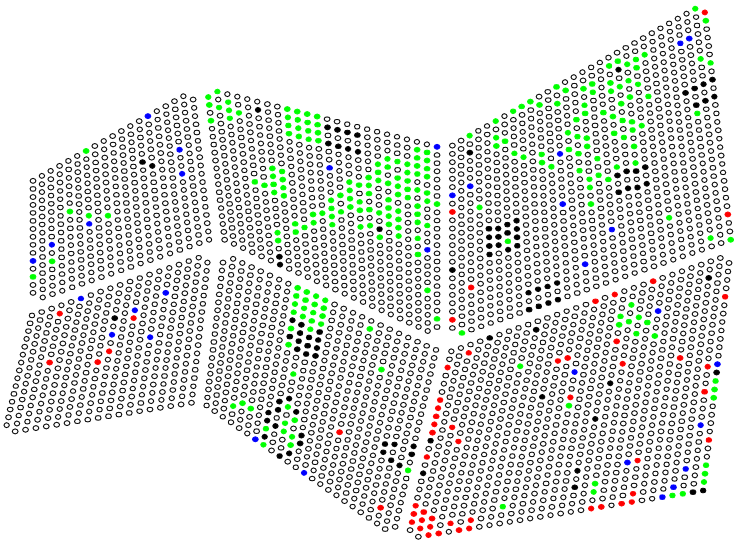

Figure 3.6: An end view of the straws in the test beam setup. Black straws have no hits in the test beam, green straws have a noise level below 0.01%. Blue straws correspond to those declared dead at the test bench, and which had a noise level below 0.01% in the considered test beam runs whereas red straws are the ones which where declared dead at the test bench, but which had a noise level above 0.01%.

to avoid e.g. voltage problems affecting other nearby channels. Investigating whether or not those straws can still give rise to noise hits in the test beam can give an indication about the nature of the noise. In figure 3.6 the channels of the test beam are shown and, in addition to pointing out the problematic channels known from the test bench, colour codes differentiate between the channels that are entirely without noise hits in the test beam, those with a very low rate of noise and the rest. The larger collection of straws entirely without hits are indeed seen to correspond nicely to non-functioning ASDBLR or DTMROC chips.[5] There is a clear correlation between the channels disconnected at the test bench and the straws that hardly if ever produce noise hits. However, the main part of them *do* produce noise hits to some degree, meaning that part of the noise is produced in the front-end chip itself.

# 4 Conclusions

Data from several runs of the summer 2004 TRT standalone test beam has been analysed. After having selected and removed a smaller number of channels with decidedly "abnormal" behaviour, the appearance and composition of the noise hits in the remaining channels have been studied and can to a large degree said to be understood. It has been shown that the composition of noise digits is very stable across the different runs and the channel-to-channel correlations between noise levels have been investigated.

[5] The eight straws connected to an ASDBLR chip are typically placed as two lines of four straws separated by one line of other straws.

## Acknowledgements

The authors wishes to express their gratitude for the many helpful comments and suggestions received by the TRT community. In particular the effort of making the test beam results easily accessible by filtering, selecting, storing and documenting the data by V. Tikhomirov was essential for the present study.

## References

[A+01] C. Alexander et al., *Progress in the development of the DTMROC time measurement chip for the ATLAS transition Radiation Tracker (TRT)*, IEEE Trans. Nucl. Sci. **48**, 514–519 (2001).

[ATL97a] ATLAS Collaboration, *ATLAS Inner Detector: Technical Design Report. Vol. 1*, (Apr 1997), CERN-LHCC-97-16.

[ATL97b] ATLAS Collaboration, *ATLAS Inner Detector: Technical Design Report. Vol. 2*, (Apr 1997), CERN-LHCC-97-17.

[B+96] B. Bevensee, F. M. Newcomer, R. Van Berg and H. H. Williams, *An amplifier shaper discriminator with baseline restoration for the ATLAS transition radiation tracker*, IEEE Trans. Nucl. Sci. **43**, 1725–1731 (1996).

[Gag05] P. Gagnon, ATLAS TRT Barrel module passports, Web interface can be found at `http://trt-wts.web.cern.ch/trt-wts/passp/bmenu.html`, 2005.

[LR04] F. Luehring and A. Romaniouk, ATLAS TRT Barrel in Test Beam, Atlas eNews, Sep 2004, `http://aenews.cern.ch/aenews.php?issueno=200409`.

[Tik04] V. Tikhomirov, Barrel TRT performance and electron/pion rejection, Talk given at ATLAS TRT Meeting, CERN, August 30, 2004.

[TRT04] T. Akesson et al. (ATLAS TRT Collaboration), *ATLAS Transition Radiation Tracker test-beam results*, Nucl. Instrum. Meth. **A522**, 50–55 (2004).